Neurobiology of Disease 110 (2018) 12–19

Contents lists available at ScienceDirect

Neurobiology of Disease

journal homepage: www.elsevier.com/locate/ynbdi

Lovastatin suppresses hyperexcitability and seizure in Angelman syndrome model

Leeyup Chung[a,1], Alexandra L. Bey[b], Aaron J. Towers[c], Xinyu Cao[a], Il Hwan Kim[d], Yong-hui Jiang[a,b,c,*]

[a] Department of Pediatrics, Duke University School of Medicine, Durham, NC 27710, United States
[b] Department of Neurobiology, Duke University School of Medicine, Durham, NC 27710, United States
[c] University Program in Genetics and Genomics, Duke University School of Medicine, Durham, NC 27710, United States
[d] Department of Cell Biology, Duke University School of Medicine, Durham, NC 27710, United States

ARTICLE INFO

Keywords:
Angelman syndrome
Ube3a
Seizure
Lovastatin
Long burst

ABSTRACT

Epilepsy is prevalent and often medically intractable in Angelman syndrome (AS). AS mouse model ($Ube3a^{m-/p+}$) shows reduced excitatory neurotransmission but lower seizure threshold. The neural mechanism linking the synaptic dysfunction to the seizure remains elusive. We show that the local circuits of $Ube3a^{m-/p+}$ *in vitro* are hyperexcitable and display a unique epileptiform activity, a phenomenon that is reminiscent of the finding in fragile X syndrome (FXS) mouse model. Similar to the FXS model, lovastatin suppressed the epileptiform activity and audiogenic seizures in $Ube3a^{m-/p+}$. The *in vitro* model of $Ube3a^{m-/p+}$ is valuable for dissection of neural mechanism and epilepsy drug screening *in vivo*.

1. Introduction

Angelman syndrome (AS) is a neurodevelopmental disorder caused by maternal deficiency of the E6-AP ubiquitin ligase (UBE3A) associated with a deletion of chromosome 15q11–q13 region, paternal uniparental disomy, point mutation in *UBE3A* or an imprinting defect (Buiting et al. 2016; Jiang et al. 1999). Clinically, epilepsy or seizure disorder is one of the most common (80 to 95%) and devastating features in AS, which starts before 3 years of age in most cases (Fiumara et al. 2010; Thibert et al. 2013). The seizure phenotype is reported to be more prominent in AS patients with a maternal deletion of chromosomal 15q11-q13 region, presumably due to the haploinsufficiency of a cluster of GABA receptors including GABRB3 in the distal end (Dan 2009; DeLorey et al. 1998; Egawa et al. 2008). The electroencephalogram (EEG) in AS patients has a characteristic pattern of large-amplitude slow-spike waves at 1–2 or 4–6 Hz (Sidorov et al. 2017; Vendrame et al. 2012). A significant fraction of clinical seizures is medically intractable and the quality of life is significantly compromised in these individuals (Tan and Bird 2016).

The epilepsy in AS is mostly generalized but partial epilepsy has also been frequently observed. The specific clinical seizures may vary from atypical absence, myoclonic, generalized tonic-clonic, tonic and atonic seizures (Dan 2009; Tan and Bird 2016). The genotype and phenotype correlation for seizure presentation has been described. Chromosomal deletion results in more severe seizure than other causes including uniparental disomy, point mutation in *UBE3A* gene, and an imprinting defect (Thibert et al. 2013). Current treatment is symptomatic with one or multiple drugs at a time. Valproic acid and clonazepam are most commonly prescribed but others such as levetiracetam, lamotrigine and clobazam have also been used frequently (Shaaya et al. 2016; Thibert et al. 2009). The molecular target therapy of reactivating *UBE3A* from the paternal chromosome has been investigated in animal model but remains to be seen if this is feasible in human (Buiting et al. 2016; Huang et al. 2012; Meng et al. 2015).

Despite the substantial progress in understanding the molecular basis and synaptic mechanism of AS, the mechanism underlying seizure caused by the *UBE3A* deficiency remains poorly understood. The AS mouse model ($Ube3a^{m-/p+}$) recapitulates the major clinical features of AS including abnormal EEG in hippocampus and neocortex (Jiang et al. 1998; Mandel-Brehm et al. 2015; Miura et al. 2002). Increased susceptibility of audiogenic seizures has been reported in AS model and they are mouse strain and age dependent (Jiang et al. 1998; Jiang et al.,

Abbreviations: AS, Angelman syndrome; BMI, (−)-bicuculline methiodide; DHPG, (*RS*)-3,5-dihydroxyphenylglycine; EEG, electroencephalogram; FXS, fragile X syndrome; LTD, long-term depression; mGluR, metabotropic glutamate receptor; MPEP, 2-Methyl-6-(phenylethynyl)pyridine hydrochloride; UBE3A, E6-AP ubiquitin ligase

* Correspondence to: Yong-hui Jiang, Division of Medical Genetics, Department of Pediatrics and Neurobiology, GSRB1 4004, DUMC, Durham, NC 27710, United States.
E-mail address: yong-hui.jiang@duke.edu (Y.-h. Jiang).
[1] Present address: Korea Brain Research Institute, 61, Cheomdan-ro, Dong-gu, Daegu, 41068, Republic of Korea.

http://dx.doi.org/10.1016/j.nbd.2017.10.016
Received 15 June 2017; Received in revised form 11 October 2017; Accepted 27 October 2017
Available online 31 October 2017
0969-9961/ © 2017 Elsevier Inc. All rights reserved.

2010; Mandel-Brehm et al. 2015). The spontaneous seizure is also observed in AS model with a maternal deletion from *Ube3a* to *Gabrb3* but at a low frequency (Jiang et al., 2010). The excitatory neurotransmission was decreased in neocortex and hippocampal CA1 region (Greer et al. 2010; Kaphzan et al. 2011; Wallace et al. 2012; Yashiro et al. 2009). The increased SK2 potassium channel levels for after-hyperpolarization in *Ube3a*$^{m-/p+}$ might suggest a decrease of excitability as well (Sun et al. 2015). Interestingly, GABAergic neuron specific loss of *Ube3a* results in abnormal EEG and enhanced seizure susceptibility (Judson et al. 2016; Santini and Klann 2016).

While these findings provide a plausible mechanistic link between the deficiency of *Ube3a* and hyperexcitability, a significant gap is present to translate this knowledge to the development of novel molecular targets for treatment of seizure. Because of the spontaneous nature of seizure activity *in vivo*, a unique local circuit phenomenon that recapitulates the hyperexcitability would be valuable for anti-seizure drug screening and understanding the epileptogenesis in AS. In this study, we attempted to delineate a hyperexcitable local circuit activity in the hippocampus of *Ube3a*$^{m-/p+}$ *in vitro*, a brain region that has been studied extensively for synaptic function and where abnormal EEG was also observed analogous to those in cortex (Greer et al. 2010; Miura et al. 2002). While the brainstem has been frequently implicated in the initiation of audiogenic seizure in rodent model, the involvement hippocampus has also been reported (Reid et al. 1983). We expect that the knowledge learned from the hippocampus of *Ube3a*$^{m-/p+}$ will be applicable to other brain regions (McNamara et al. 2006). In this study, we demonstrate the value of this platform for the development of anti-epileptic drugs for AS.

2. Materials and methods

2.1. Animals

All experiments were conducted according to the protocols approved by the Institutional Animal Care and Use Committee at Duke University. Animals were housed on a 12 h light/dark cycle. Mice of *Ube3a*$^{m+/p+}$ and *Ube3a*$^{m-/p+}$ were produced from breedings between *Ube3a*$^{m+/p-}$ females and wild-type C57BL/6 males. Littermates were used as controls for all experiments. Primers used for genotyping are as following: P1/genomic forward, 5′-CTTCTCAAGGTAAGCTGAGCTTGC-3′, P2/reverse, 5′-GCTCAAGGTTGTATGCCTTGGTGCT-3′ and P3/HPRT forward, 5′-TGCATCGCATTGTGTGAGTAGGTGTC-3′. PCR cycle conditions were 95 °C for 30 s, 56 °C for 60 s and 70 °C for 45 s for 35 cycles.

2.2. Brain slice preparation

Transverse hippocampal slices (400 μm) were prepared from postnatal day (P)17-P27 mice for excitability experiments or from P20 to P35 mice for LTD (long-term depression) experiments. For LTD experiments, CA3 was removed. Ice cold slicing solution contained in mM: 75 sucrose, 87 NaCl, 2.5 KCl, 1.25 NaH_2PO_4, 26 $NaHCO_3$, 10 glucose, 7 $MgCl_2$, 0.5 $CaCl_2$. Slices were recovered at room temperature (Fig. 1) or at 30 °C (Figs. 2 and 3) for at least 2 h in artificial cerebrospinal fluid (ACSF). ACSF contained in mM: 124 NaCl, 3 KCl, 1.25 NaH_2PO_4, 26 $NaHCO_3$, 10 glucose, 1 $MgCl_2$, and 2 $CaCl_2$.

2.3. Field potential recording

Hippocampal slices were placed in the submersion chamber maintained at 30 °C. After acclimation period (> 30 min), glass recording electrodes (1–3 MΩ) filled with ACSF, were placed in CA1 or CA3 pyramidal layer. For trains of stimulation experiment, stimulating electrode was placed at the border between CA1 and CA3. Vehicle or drugs were bath applied. The input-output relationship was obtained by 5, 10, 15, 20, 25, 30, 40, 50, 60, 100 μA stimulation (200 μsec, DS301 or Isoflex). Paired-pulse ratios were obtained from the ratio of the second field excitatory postsynaptic potential (fEPSP) slope to the first, for a range of inter-stimulus intervals (25–2000 ms). For LTD, *(RS)*-3,5-dihydroxyphenylglycine (DHPG) (100 μM, 10 min) was applied after stable baseline for 20 min (< 5% drift). The slope at 55–60 min was compared to the pre-conditioning baseline response (last 5 min of baseline).

The criteria for the "long burst" in this study was set at burst duration of longer than 2 s. This is based on the previous studies where "short discharges" (interictal-like activity) is hardly longer than 1.5 s and "prolonged synchronized discharges" in stable condition (30 to 60 min after DHPG) is longer than 2 s (Chuang et al. 2005; Taylor et al. 1995; Zhao et al. 2004). The duration measurement in extracellular recording in this study is based on extracellular and intracellular recordings in previous "prolonged synchronized discharges" studies (Taylor et al. 1995; Young et al. 2013). In Fig. 3**H** and **L**, the duration of individual long bursts were averaged for each slices for the mean duration of 10 min interval. If no long bursts were present within the interval in a slice, zero was assigned.

2.4. Drug treatment

Lovastatin (sodium salt) were obtained from Millipore. (*RS*)-3,5-Dihydroxyphenylglycine (DHPG), 2-Methyl-6-(phenylethynyl)pyridine hydrochloride (MPEP) and (−)-bicuculline methiodide (BMI) and nimodipine were acquired from Tocris Bioscience. Other chemicals were from Sigma. All drugs were bath applied. Extracellular K^+ concentration was raised by adding 1.0 M KCl stock solution to ACSF.

2.5. Lovastatin treatment and audiogenic seizure

Mice of P15 to P23 were injected i.p. with: (1) 10 mg/kg lovastatin acid or vehicle (DMSO 100%); (2) 100 mg/kg lovastatin acid or vehicle (DMSO 100%). Mice were housed in home cage for one hour before evoking audiogenic seizure. Each mouse was transferred to a plastic test chamber (17 × 22 × 20 cm) and habituated for 1 min. A loud sound (about 130 dB) was generated for 2 min from a personal alarm (Radioshack model 49-1010). The behavior was monitored with digital video camera recorder (Sony DCR-SR45). The positive for seizure was scored only when tonic-clonic movement was observed (van Woerden et al. 2007).

2.6. Statistical analysis

Fisher's exact test (two-tailed) for categorical data, *t*-test and paired *t*-test for independent and repeated two group comparisons and repeated one-way ANOVA with Tukey post-hoc test for 3 repeated measurements were used. The level of significance was set at $p < 0.05$.

3. Results

3.1. Lower threshold for hyperexcitability in *Ube3a*$^{m-/p+}$ brain slices

Ube3a$^{m-/p+}$ mice displayed a lower threshold for audiogenic seizures (Jiang et al. 1998; Mandel-Brehm et al. 2015; Miura et al. 2002; van Woerden et al. 2007). This would predict that the neuronal circuit in *Ube3a*$^{m-/p+}$ has higher excitability than wild type (*Ube3a*$^{m+/p+}$) in *in vitro* model. Because the abnormal EEG and abnormal synaptic function has been well characterized in hippocampus of AS model (Miura et al. 2002), we monitored the neuronal excitability in the CA1 of *Ube3a*$^{m-/p+}$ bran slices in response to the sequential increase of extracellular K^+ ion concentration (Fig. 1**A–B**). The experimenter was blind to the genotypes in the experiments where both wild type and *Ube3a*$^{m-/p+}$ were used. At 6 mM of K^+, 4 of 7 *Ube3a*$^{m-/p+}$ brain slices (one slice per mouse) showed synchronized discharges but none of *Ube3a*$^{m+/p+}$ (0 of 6 slices, 6 mice) (Fisher's exact test, $p = 0.025$). The number of synchronized discharges within the 20 min observation

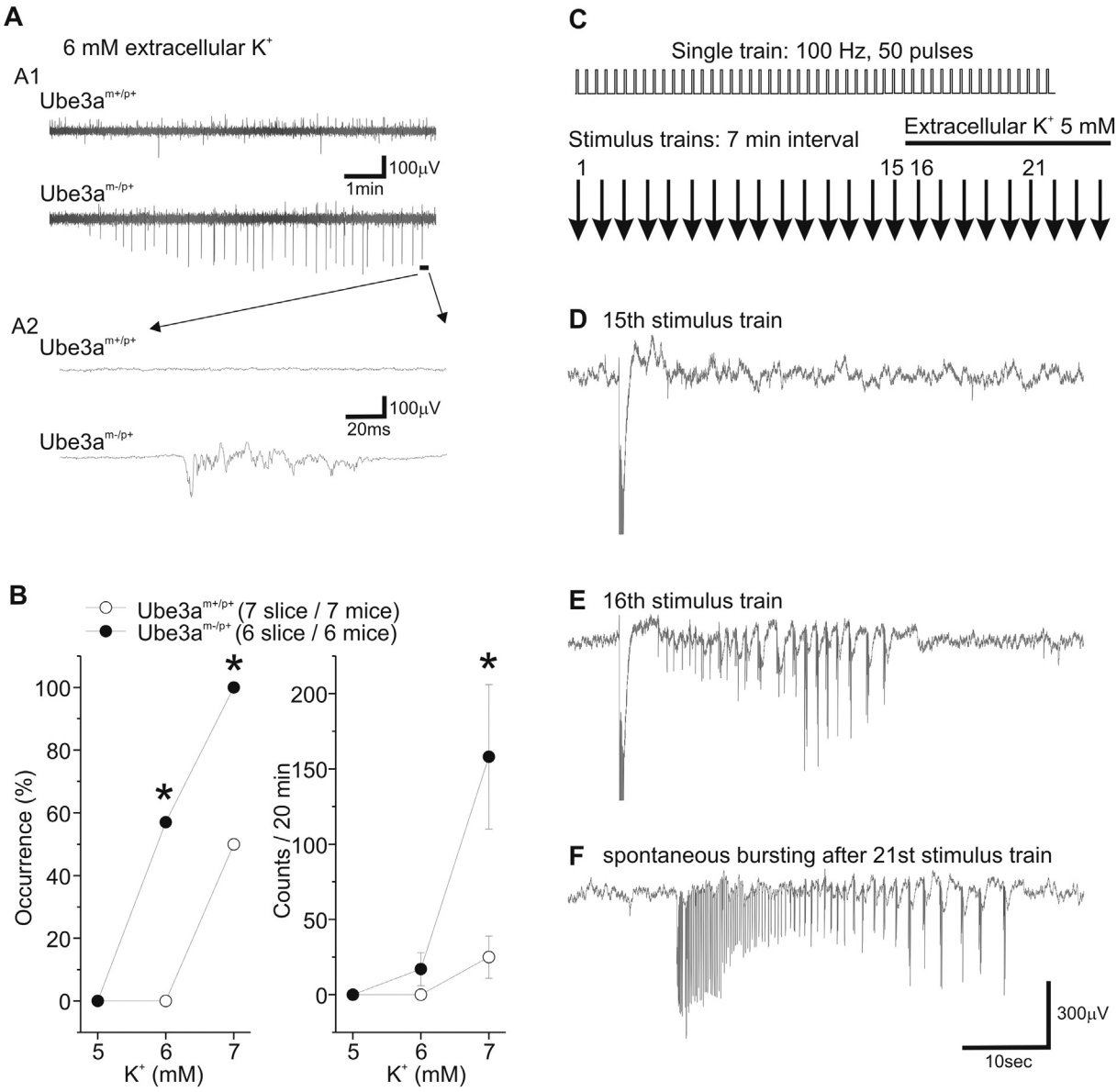

Fig. 1. Hyperexcitability in *Ube3a*$^{m-/p+}$ hippocampal slices.
A, A1. A representative trace of synchronized activity at 6 mM extracellular K^+ concentration in a *Ube3a*$^{m+/p+}$ or *Ube3a*$^{m-/p+}$ slice. A2. Expanded trace of marked part in A1. **B,** Synchronized activity occurrence ratio (left) and the number of individual activities (right). **C–F,** The traces of synchronized rhythmic discharges (seizure-like activity) in an *Ube3a*$^{m-/p+}$ slice upon electrical stimulation. (**C**) The electrical stimulation protocol to Schaffer collaterals in hippocampus (one train = 50 stimulations at 100 Hz, train interval = 7 min). After the 15th train **(D)** extracellular K^+ concentration was raised from 3 to 5 mM. (**E**) Synchronized rhythmic discharges after the 16th train. (**F**) An example of spontaneous burst activity. $^*p < 0.05$.

period was higher in *Ube3a*$^{m-/p+}$ at 7 mM (*Ube3a*$^{m+/p+}$, 25 ± 14 *vs* *Ube3a*$^{m-/p+}$, 158 ± 48; $p = 0.031$, two-tailed *t*-test) (Fig. 1**B**).

Next we tested whether the neural circuit in *Ube3a*$^{m-/p+}$ brain slices was more excitable in response to the synaptic inputs by trains of electrical stimulation (Isomura et al. 2008; Stasheff et al. 1989). The stimuli were applied to the Schaffer collaterals with a recording electrode in the CA1 pyramidal layer (Fig. 1**C**). In ACSF with 3 mM K^+, the stimulus did not evoke synchronized rhythmic discharges. At the end of 15th train, the extracellular K^+ was raised to 5 mM. In this condition all *Ube3a*$^{m-/p+}$ slices showed synchronized rhythmic discharges while none of the *Ube3a*$^{m+/p+}$ slices displayed similar activities (*Ube3a*$^{m-/p+}$, 5 of 5 slices, one slice per mouse; *Ube3a*$^{m+/p+}$, 0 of 5 slices, one slice per mouse; $p = 0.008$, Fisher's exact test) (Fig. 1**D–F**).

3.2. *Ube3a*$^{m-/p+}$ *CA3 displayed long burst activity*

In presence of the $GABA_A$ receptor antagonist, bicuculline (BMI), brief synchronized activities were observed in CA3 of both *Ube3a*$^{m+/p+}$ and *Ube3a*$^{m-/p+}$ brain slices. However, *Ube3a*$^{m-/p+}$ slices exhibited additional long burst activity in 6 of 7 slices (5 mice) while none of *Ube3a*$^{m+/p+}$ slices did (7 slices, 5 mice) ($p = 0.005$, Fisher's exact test; Fig. 2**A–C**). As a preliminary test of similarity between the long burst in our study and those in previous studies mediated by group I metabotropic glutamate receptor, we applied mGluR5 antagonist (Taylor et al. 1995; Zhao et al. 2004). Application of MPEP (50 μM), an mGluR5 antagonist, suppressed the long burst activity completely in duration (sec) and occurrence (counts/10 min) (*Ube3a*$^{m-/p+}$, 3 slices, 3 mice; duration (sec), 6.9 ± 0.4 *vs* 0.0 ± 0.0, $p = 0.003$; counts/10 min, 3.2 ± 0.3 *vs* 0 ± 0, p = 0.008, 2 tailed and paired *t*-test, before *vs* after MPEP; Fig. 2**D–E**).

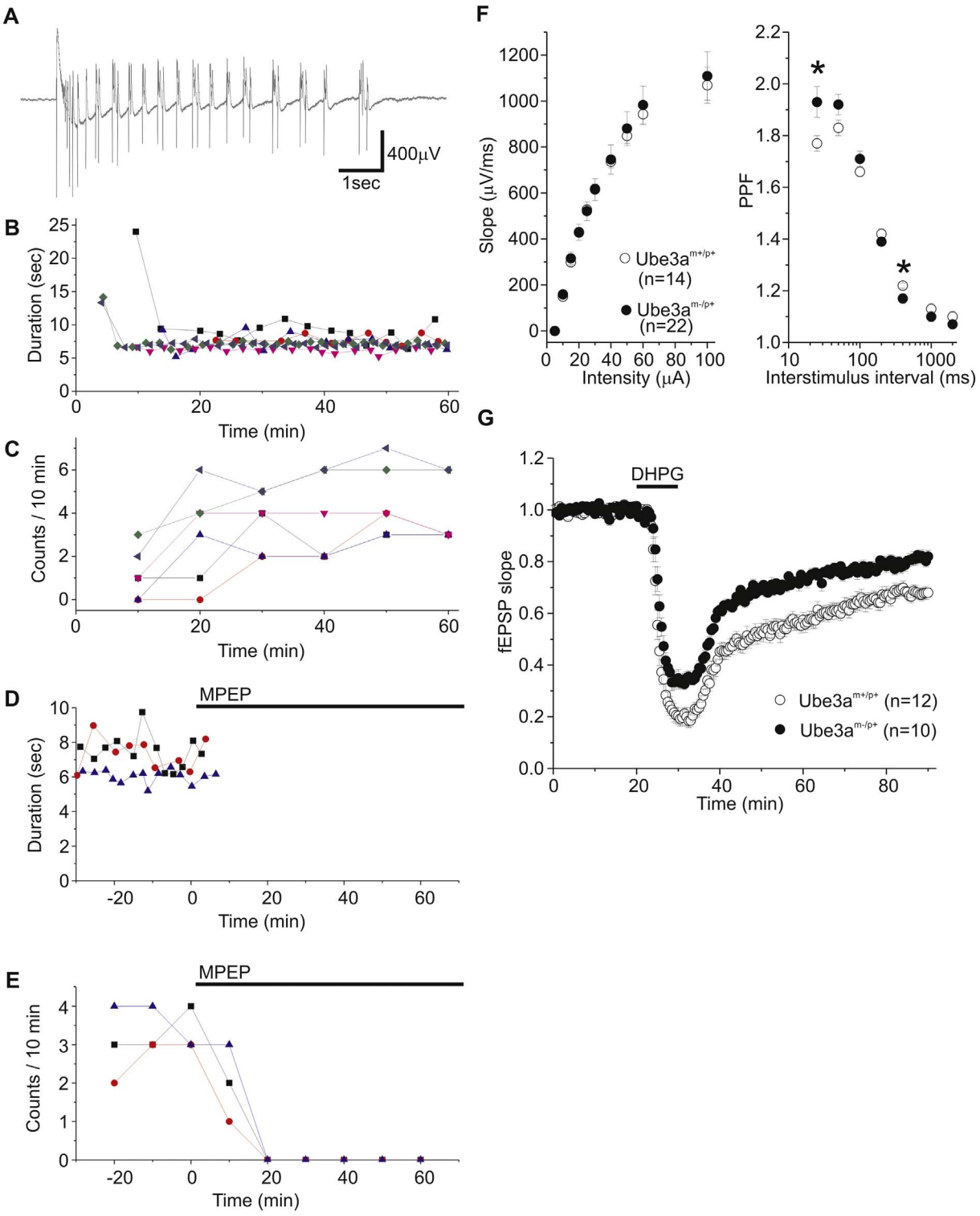

Fig. 2. Spontaneous long bursts in response to BMI treatment and reduced DHPG-LTD in hippocampus of *Ube3a*$^{m-/p+}$ mice.
A, A representative trace of long burst activity from a *Ube3a*$^{m-/p+}$ slice in 5 mM K^+ and BMI (50 μM). The duration (**B**) and frequency (**C**) of long bursts per 10 min from each *Ube3a*$^{m-/p+}$ slices (n = 6; different symbols for each slices). **D–E,** MPEP (50 μM) blocked long bursts in duration (**D**) and frequency (**E**) (n = 3; different symbols for each slices). **F,** The input-output relationship (left) and paired pulse facilitation (right) were similar between *Ube3a*$^{m+/p+}$ and *Ube3a*$^{m-/p+}$. **G,** The DHPG induced LTD was reduced in *Ube3a*$^{m-/p+}$. DHPG (100 μM, 10 min). *p < 0.05.

3.3. Hippocampal group I mGluR dependent long-term depression (LTD) is reduced in *Ube3a*$^{m-/p+}$ mice

A similar type of long burst activity in hippocampal slice has been reported in fragile X syndrome (FXS) mouse model (Chuang et al. 2005; Young et al. 2013). We then tested if the similarity of long burst activity between *Ube3a*$^{m-/p+}$ and FXS model extended to synaptic plasticity of LTD that is enhanced in CA1 synapses in FXS model (Huber et al., 2002). The basal synaptic transmissions were similar between *Ube3a*$^{m-/p+}$ and *Ube3a*$^{m+/p+}$ mice (Fig. 2**F**). Contrary to our

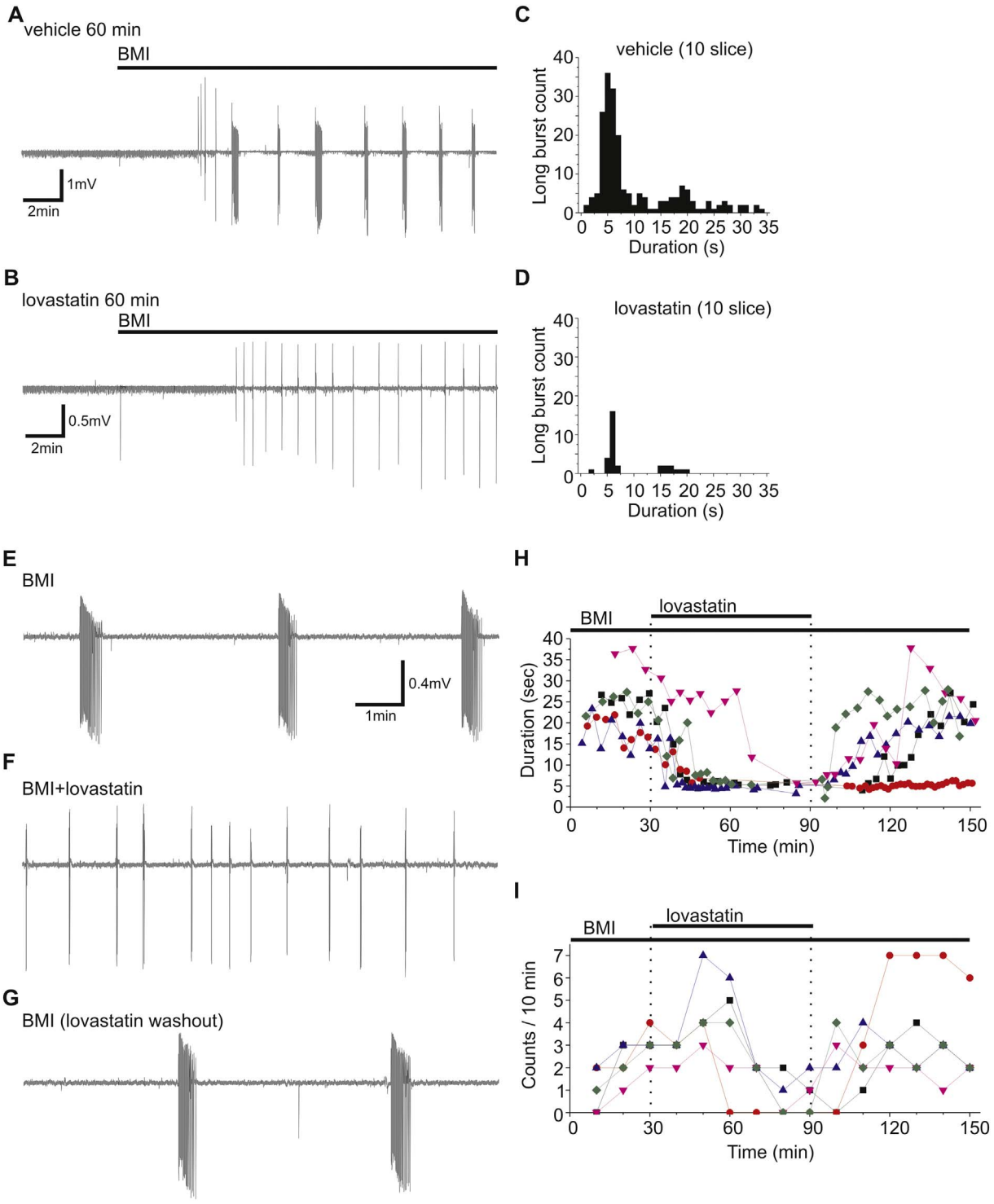

Fig. 3. Lovastatin inhibited long bursts in hippocampal slices of *Ube3a*$^{m-/p+}$.
A–B, Pre-treatment (60 min) of vehicle (DMSO) or lovastatin (50 μM) before BMI. **C–D,** Summary of long burst duration in vehicle treatment group (C, *Ube3a*$^{m-/p+}$) and in lovastatin treatment group (D, *Ube3a*$^{m-/p+}$). **E–G**. A representative trace of long burst activity from a *Ube3a*$^{m-/p+}$ hippocampus slice in response to the treatment of BMI (**E**), lovastatin (**F**) and lovastatin washout (**G**). **H–I**. The duration (**H**) and frequency (**I**) of long bursts per 10 min from each *Ube3a*$^{m-/p+}$ hippocampus slices during the treatment of BMI, lovastatin and lovastatin washout (n = 5; different symbols for each slices). **J–K**. Long bursts in BMI right before nimodipine (J) and absence of long bursts after nimodipine (10 μM) in an *Ube3a*$^{m-/p+}$ slice. **L–M**. The duration (**L**) and frequency (**M**) of long bursts per 10 min from each slices (n = 7; different symbols for each slices).

expectation, group I mGluR dependent LTD was decreased in *Ube3a*$^{m-/p+}$ (*Ube3a*$^{m+/p+}$, 68 ± 2%, n = 12; *Ube3a*$^{m-/p+}$, 81 ± 2%, n = 10, $p < 0.001$, 2-tailed *t*-test) (Fig. 2**G**). These results indicate that AS and FXS mouse models may share the mechanism for hyperexcitability but not for the synaptic plasticity. In the FXS model, the excessive protein synthesis in synapses is the major mechanism underlying the enhanced LTD while mechanism for impaired LTD in AS model is not immediately clear.

3.4. Lovastatin suppressed long bursts in brain slices of *Ube3a*$^{m-/p+}$ mice

Lovastatin (Statin), a common drug used for lowering cholesterol,

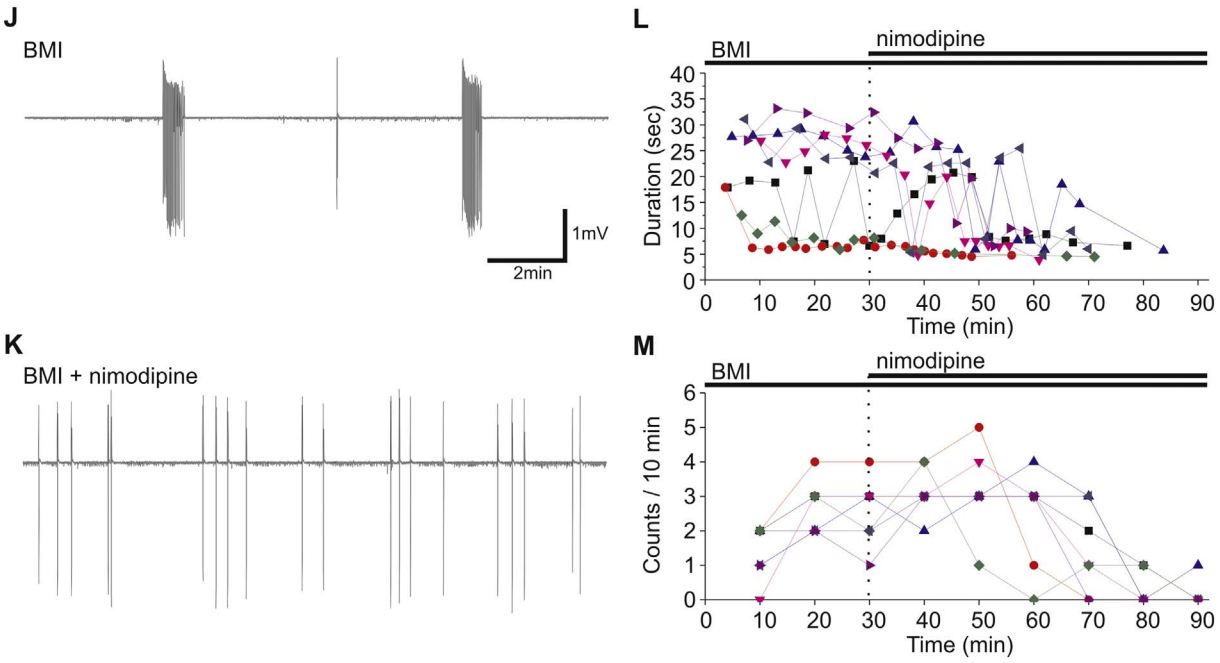

Fig. 3. (*continued*)

has been shown to suppress the generation of long bursts *via* the inhibition of excessive protein synthesis in hippocampus of FXS mouse model (Osterweil et al. 2013). We then tested if lovastatin pre-treatment can prevent the generation of long bursts in *Ube3a*$^{m-/p+}$ mice as well. With vehicle pre-treatment, BMI evoked long bursts in 9 of 10 slices in *Ube3a*$^{m-/p+}$ within the 60 min recording time (n = 199 bursts, 6 mice; Fig. 3**A–B**). However, with lovastatin pre-treatment, the long burst activity did not occur at all in 7 of 10 *Ube3a*$^{m-/p+}$ slices (6 mice; $p = 0.020$, Fisher's exact test, vehicle *vs* lovastatin; Fig. 3**C**). In the remaining 3 slices with occurrence of long bursts (n = 32 bursts), the latency to the first long burst was significantly delayed (vehicle, 394.74 ± 38.44 s, n = 9 slices; lovastatin, 1566.65 ± 605.10 s, n = 3 slices; $p = 0.004$, 2-tailed *t*-test; Fig. 3**D**). However, the duration of long bursts was not different from that of vehicle condition (vehicle, 9.98 ± 0.55 s, n = 199 bursts, 9 slices *vs* lovastatin, 8.84 ± 0.94 s, n = 32 bursts, 3 slices; $p = 0.423$, 2-tailed *t*-test).

In FXS model, the suppression of long bursts by lovastatin is proposed to be mediated by the inhibition of excessive protein synthesis at synapses. The observed effect of lovastatin in AS model prompted us to assess whether the similar mechanism may operate in AS model. Previous studies have shown that once long bursts were induced by the group I mGluR agonist (DHPG), they could not be inhibited by protein synthesis inhibitors or lovastatin (Merlin et al. 1998; Osterweil et al. 2013). This observation supports that protein synthesis is required for the generation of long burst, but not for the maintenance afterwards. Interestingly, in AS model, when lovastatin was applied after the occurrence of long bursts in *Ube3a*$^{m-/p+}$ slices, lovastatin could still effectively suppress long bursts (Fig. 3**E**). The long burst returned during the washout period of lovastatin (10 min before lovastatin: 23.354 ± 3.606 s, 50 to 60 min after lovastatin: 3.141 ± 1.316 s, 50 to 60 min washout of lovastatin: 19.942 ± 3.641 s; before *vs* after, $p < 0.001$; after *vs* washout, $p = 0.001$; repeated one-way ANOVA, Tukey post-hoc test, n = 5 slices from 3 mice; Fig. 3**H**). The frequency of long burst followed similar pattern as duration but the difference was at borderline (10 min before lovastatin: 3.0 ± 0.3, 50 to 60 min after lovastatin: 0.8 ± 0.4, 50 to 60 min washout of lovastatin: 2.8 ± 0.8; before *vs* after, $p = 0.050$; after *vs* washout, $p = 0.073$; repeated one-way ANOVA, Tukey post-hoc test, n = 5 slices from 3 mice; Fig. 3**I**). This result suggest that a different mechanism other than protein synthesis inhibition may be responsible for the lovastatin effect in the AS model.

The anticonvulsant effect of lovastatin and its analogs has been investigated in many different seizure models in rodent and a few observational studies in human (Banach et al. 2014; Russo et al. 2013). While the efficacy has been demonstrated in some of these models, the mechanism is unknown. In survey of the data in literature to understand the effect of lovastatin in AS model, we noted a report that lovastatin may act as an L-type calcium channel blocker (Bergdahl et al. 2003). The involvement of L-type calcium channel in epilepsy and the anticonvulsant effect of the antagonist have been reported (Nicita et al. 2016; Rajakulendran and Hanna 2016). To test if antagonizing L-type calcium channels can suppress the long burst, we chose nimodipine, which is in clinical use for hypertension and in human epilepsy by the case report (Nicita et al. 2016; Zamponi et al. 2015). In *Ube3a*$^{m-/p+}$ slices, nimodpine (10 μM) suppressed the pre-existing long busts after BMI (mean duration, 10 min before nimodipine: 18.884 ± 3.724 s *vs* 50 to 60 min after nimodipine: 0.813 ± 0.813 s, $p = 0.002$; mean frequency, 10 min before nimodipine: 2.6 ± 0.4 *vs* 50 to 60 min after nimodipine: 0.1 ± 0.1, $p < 0.001$; paired *t*-test, n = 7 slice, 5 mice; Fig. 3**J–M**).

3.5. Lovastatin suppressed audiogenic seizures in *Ube3a*$^{m-/p+}$ mice

We tested if lovastatin can prevent seizure generation in *Ube3a*$^{m-/p+}$ mice as in the FXS mouse model (Osterweil et al. 2013). At single dose of 10 mg/kg by intraperitoneal (i.p.) injection, the rate of seizure induction in *Ube3a*$^{m-/p+}$ was comparable between lovastatin treated (3 of 12) and vehicle treated group (5 of 12, $p = 0.667$, Fisher's exact test) (Fig. 4**A**). *Ube3a*$^{m+/p+}$ mice did not show seizure in either vehicle (0 of 7) nor in lovastatin (0 of 8). At single dose of 100 mg/kg, the rate of seizure induction was reduced in lovastatin treated *Ube3a*$^{m-/p+}$ mice (1 of 18) compared with in vehicle (8 of 18; $p = 0.018$, Fisher's exact test) (Fig. 4**B**). *Ube3a*$^{m+/p+}$ did not show seizures in vehicle (0 of 15) nor in lovastatin (0 of 15).

4. Discussion

We successfully established an *in vitro* cellular model that recapitulates the hyperexcitability *in vivo* in an AS *Ube3a*$^{m-/p+}$ mouse model. *Ube3a* maternal deficient local circuitry is hyperexcitable in

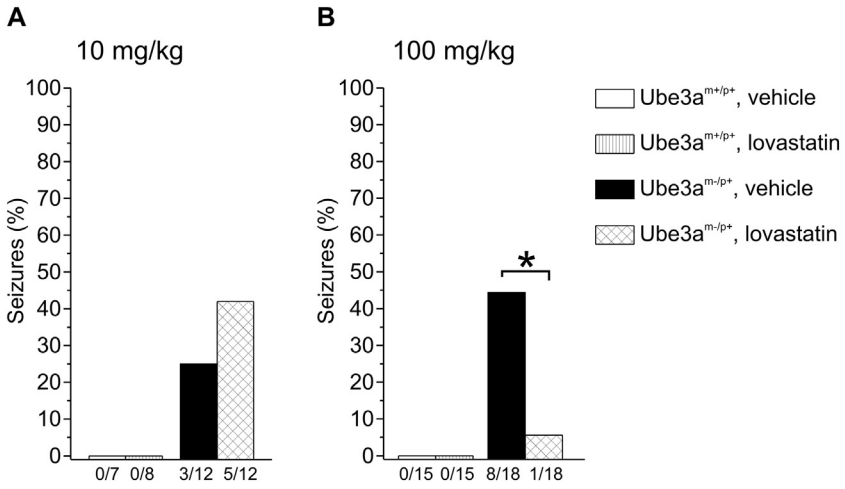

Fig. 4. Lovastatin treatment inhibited audiogenic seizures in *Ube3a*$^{m-/p+}$ mice.
A, Low dose of lovastatin treatment (10 mg/kg) did not have significant seizure suppression effect in *Ube3a*$^{m-/p+}$ mice (*Ube3a*$^{m+/p+}$, vehicle, n = 7 mice; *Ube3a*$^{m+/p+}$, lovastatin n = 8 mice; *Ube3a*$^{m-/p+}$, vehicle, n = 12 mice; *Ube3a*$^{m-/p+}$, lovastatin, n = 12 mice). **B,** High dose of lovastatin treatment (100 mg/kg) significantly suppressed the audiogenic seizure in *Ube3a*$^{m-/p+}$ mice (*Ube3a*$^{m+/p+}$, vehicle, n = 15 mice; *Ube3a*$^{m+/p+}$, lovastatin n = 15 mice; *Ube3a*$^{m-/p+}$, vehicle, n = 18 mice; *Ube3a*$^{m-/p+}$, lovastatin, n = 18 mice). *p < 0.05.

hippocampal slice preparation in response to the increase in the extracellular K^+ as well as to strong synaptic input evoked by the electrical stimulation protocol. The hyperexcitability in hippocampal slices is consistent with the abnormal EEG reported in AS *Ube3a*$^{m-/p+}$ mouse model *in vivo* (Miura et al. 2002). Thus, the brain slice preparation is valuable to dissect the mechanism underlying the seizure susceptibility; more importantly, it provides a unique and valuable platform for the test of anti-epilepsy drugs in AS.

We unexpectedly uncovered the similarity for the local circuit activities between AS and FXS mouse models. The long burst activity induced by BMI in CA3 of *Ube3a*$^{m-/p+}$ mice was very similar to that observed in FXS mouse model (Chuang et al. 2005). Because epilepsy and seizures are also frequent features in the FXS (Contractor et al. 2015; Heard et al. 2014; Musumeci et al. 1999; Thomson et al. 2017), our observations suggest a shared mechanism underlying the susceptibility to seizures in both models. The same response to the lovastatin treatment in both models supports this conclusion. However, we found the synaptic plasticity measured by DHPG-LTD in *Ube3a*$^{m-/p+}$ is altered in opposite direction to that of FXS mouse model (Huber et al., 2002). This may argue that the signaling pathway for DHPG-LTD may not be implicated in the hyperexcitability of both models. Consistent with this, it has been shown that the genetic manipulation of Homer1a in FXS model could correct the hyperexcitability but not the DHPG-LTD (Ronesi et al. 2012).

In the FXS model, the inhibition of excessive protein synthesis is shown to be responsible for the effect of lovastatin treatment (Osterweil et al. 2013). This is consistent with observation that the long burst or epileptiform activity is dependent on increased group I mGluR pathway in the FXS model (Hays et al. 2011; Osterweil et al. 2013; Zhao et al. 2015). Once induced by DHPG, the prolonged bursts could not be inhibited by protein synthesis inhibitor or lovastatin (Merlin et al. 1998; Merlin and Wong 1997; Osterweil et al. 2013). In contrast, lovastatin was able to suppress the existing long bursts in AS *Ube3a*$^{m-/p+}$ mice. These observations do not provide immediate support that the excessive protein synthesis is responsible for the effect of lovastatin treatment in AS model.

Biochemically, UBE3A is known to be an ubiquitin E3 ligase that involves the proteasome mediated protein degradation (Scheffner et al. 1993). The increase of synaptic proteins resulting from the deficiency of UBE3A has been reported in AS model (Sell and Margolis 2015). Therefore, it can be hypothesized that lovastatin may modulate the upregulated protein functions in AS model by a mechanism other than protein synthesis inhibition. Suppression of long burst by nimodipine in AS model suggest that lovastatin may have additional role as an L-type calcium channel modulator. The L-type calcium channel has been implicated in epilepsy and seizure disorders (Stiglbauer et al. 2017; Zamponi et al. 2015). Further study to examines whether the L-type calcium channels is dysregulated molecularly in AS model is warranted.

The study of other alternative mechanism may also be pursued to understand the shared mechanism of hyperexcitability between AS and FXS models. A direct interaction between FMRP and UBE3A has been suggested as *Ube3a* is one of the mRNA targets of FMRP (Ascano et al. 2012). The involvement of Arc protein has also been implicated in both AS and FXS model. Increased Arc protein level is found in the hippocampus of AS model (Greer et al. 2010; Kuhnle et al. 2013) while the reduction of Arc protein by genetic manipulation in AS model lowered the seizure-like activity (Mandel-Brehm et al. 2015). In the FXS model, the deficiency of FMRP also results in the increased Arc level in dendritic spines due to the lack of FMRP-mediated inhibition of protein translation (Niere et al. 2012; Park et al. 2008). However, it is unclear whether the increased in Arc is responsible for seizure phenotype in FXS model. Further investigation is warranted to understand whether the increase of Arc may contribute to the long burst and lovastatin effect in *Ube3a*$^{m-/p+}$ mice.

It should be noted that the anticonvulsant effect of lovastatin is not unique to FXS and AS models. The studies of lovastatin and its analogs have been reported in several seizure models including audiogenic models in rodent and several observational studies in human (Banach et al. 2014; Citraro et al. 2014; Russo et al. 2013; Scicchitano et al. 2015). While the efficacy of seizure suppression varies from study to study, the anticonvulsant effect has been documented for lovastatin and other analogs. In many cases, the efficacy is related to the type of seizures presented in the models. The mechanism underlying the seizure suppression effect in these models has not been investigated. It is conceivable that multiple independent mechanisms may be responsible. We believe our report and others from FXS model provide a molecular framework for more extensive investigation of general anticonvulsant effect for lovastatin and other analogs.

In summary, the local circuit activities described in this study will facilitate the study on the molecular and cellular mechanism for epileptogenesis in *Ube3a*$^{m-/p+}$. For example, manipulations on specific Ube3a substrates or certain GABAergic interneuron types can change the quantitative properties of long burst. The understanding on the mechanism will enhance the merit of using this *in vitro* model for additional anti-epilepsy drug screen. Even before the complete understanding of epileptogenesis, the efficacy of lovastatin treatment from *in vitro* brain slice and *in vivo* in *Ube3a*$^{m-/p+}$ support an immediate translational value of this discovery as in FXS case (Caku et al. 2014). Because the reported difference for the seizure presentation between AS with point mutations in UBE3A and chromosomal deletion of 15q11-q13 (Buiting et al. 2016; Moncla et al. 1999), the replication and comparison of these findings from the *Ube3a*$^{m-/p+}$ in the AS model with a large deletion is warranted in future study (Jiang et al., 2010).

Acknowledgments

We thank Dr. Victor Nadler, Dr. Ramona Rodriguiz and Yoonji Lee for technical help. This study was supported by the grant from Angelman Syndrome Foundation and the National Institute of Health Grant MH098114, HD077197, and MH104316 for YHJ.

Conflicts of interest

The authors declare no competing financial interests.

References

Ascano Jr., M., et al., 2012. FMRP targets distinct mRNA sequence elements to regulate protein expression. Nature 492, 382–386.
Banach, M., et al., 2014. Statins - are they anticonvulsant? Pharmacol. Rep. 66, 521–528.
Bergdahl, A., et al., 2003. Lovastatin induces relaxation and inhibits L-type Ca(2 +) current in the rat basilar artery. Pharmacol. Toxicol. 93, 128–134.
Buiting, K., et al., 2016. Angelman syndrome - insights into a rare neurogenetic disorder. Nat. Rev. Neurol. 12, 584–593.
Caku, A., et al., 2014. Effect of lovastatin on behavior in children and adults with fragile X syndrome: an open-label study. Am. J. Med. Genet. A 164a, 2834–2842.
Chuang, S.C., et al., 2005. Prolonged epileptiform discharges induced by altered group I metabotropic glutamate receptor-mediated synaptic responses in hippocampal slices of a fragile X mouse model. J.Neurosci. 25, 8048–8055.
Citraro, R., et al., 2014. Protective effects of some statins on epileptogenesis and depressive-like behavior in WAG/Rij rats, a genetic animal model of absence epilepsy. Epilepsia 55, 1284–1291.
Contractor, A., et al., 2015. Altered neuronal and circuit excitability in fragile X syndrome. Neuron 87, 699–715.
Dan, B., 2009. Angelman syndrome: current understanding and research prospects. Epilepsia 50, 2331–2339.
DeLorey, T.M., et al., 1998. Mice lacking the beta3 subunit of the GABAA receptor have the epilepsy phenotype and many of the behavioral characteristics of Angelman syndrome. J. Neurosci. 18, 8505–8514.
Egawa, K., et al., 2008. Aberrant somatosensory-evoked responses imply GABAergic dysfunction in Angelman syndrome. NeuroImage 39, 593–599.
Fiumara, A., et al., 2010. Epilepsy in patients with Angelman syndrome. Ital. J. Pediatr. 36, 31.
Greer, P.L., et al., 2010. The Angelman syndrome protein Ube3A regulates synapse development by ubiquitinating arc. Cell 140, 704–716.
Hays, S.A., et al., 2011. Altered neocortical rhythmic activity states in Fmr1 KO mice are due to enhanced mGluR5 signaling and involve changes in excitatory circuitry. J. Neurosci. 31, 14223–14234.
Heard, T.T., et al., 2014. EEG abnormalities and seizures in genetically diagnosed fragile X syndrome. Int. J. Dev. Neurosci. 38, 155–160.
Huang, H.S., et al., 2012. Topoisomerase inhibitors unsilence the dormant allele of Ube3a in neurons. Nature 481, 185–189.
Huber, K.M., et al., 2002. Altered synaptic plasticity in a mouse model of fragile X mental retardation. Proc. Natl. Acad. Sci. U. S. A. 99, 7746–7750.
Isomura, Y., et al., 2008. A network mechanism underlying hippocampal seizure-like synchronous oscillations. Neurosci. Res. 61, 227–233.
Jiang, Y.H., et al., 1998. Mutation of the Angelman ubiquitin ligase in mice causes increased cytoplasmic p53 and deficits of contextual learning and long-term potentiation. Neuron 21, 799–811.
Jiang, Y., et al., 1999. Genetics of Angelman syndrome. Am. J. Hum. Genet. 65, 1–6.
Jiang, Y.H., et al., 2010. Altered ultrasonic vocalization and impaired learning and memory in Angelman syndrome mouse model with a large maternal deletion from Ube3a to Gabrb3. PLoS.One. 5.
Judson, M.C., et al., 2016. GABAergic Neuron-Specific Loss of Ube3a causes Angelman syndrome-like EEG abnormalities and enhances seizure susceptibility. Neuron 90, 56–69.
Kaphzan, H., et al., 2011. Alterations in intrinsic membrane properties and the axon initial segment in a mouse model of Angelman syndrome. J. Neurosci. 31, 17637–17648.
Kuhnle, S., et al., 2013. Role of the ubiquitin ligase E6AP/UBE3A in controlling levels of the synaptic protein Arc. Proc. Natl. Acad. Sci. U. S. A. 110, 8888–8893.
Mandel-Brehm, C., et al., 2015. Seizure-like activity in a juvenile Angelman syndrome mouse model is attenuated by reducing Arc expression. Proc. Natl. Acad. Sci. U. S. A. 112, 5129–5134.
McNamara, J.O., et al., 2006. Molecular signaling mechanisms underlying epileptogenesis. Sci. STKE 2006 (re12).
Meng, L., et al., 2015. Towards a therapy for Angelman syndrome by targeting a long noncoding RNA. Nature 518, 409–412.
Merlin, L.R., Wong, R.K., 1997. Role of group I metabotropic glutamate receptors in the patterning of epileptiform activities in vitro. J. Neurophysiol. 78, 539–544.
Merlin, L.R., et al., 1998. Requirement of protein synthesis for group I mGluR-mediated induction of epileptiform discharges. J. Neurophysiol. 80, 989–993.
Miura, K., et al., 2002. Neurobehavioral and electroencephalographic abnormalities in Ube3a maternal-deficient mice. Neurobiol. Dis. 9, 149–159.
Moncla, A., et al., 1999. Phenotype-genotype correlation in 20 deletion and 20 non-deletion Angelman syndrome patients. Eur. J. Hum. Genet. 7, 131–139.
Musumeci, S.A., et al., 1999. Epilepsy and EEG findings in males with fragile X syndrome. Epilepsia 40, 1092–1099.
Nicita, F., et al., 2016. The possible use of the L-type calcium channel antagonist verapamil in drug-resistant epilepsy. Expert. Rev. Neurother. 16, 9–15.
Niere, F., et al., 2012. Evidence for a fragile X mental retardation protein-mediated translational switch in metabotropic glutamate receptor-triggered Arc translation and long-term depression. J. Neurosci. 32, 5924–5936.
Osterweil, E.K., et al., 2013. Lovastatin corrects excess protein synthesis and prevents epileptogenesis in a mouse model of fragile X syndrome. Neuron 77, 243–250.
Park, S., et al., 2008. Elongation factor 2 and fragile X mental retardation protein control the dynamic translation of Arc/Arg3.1 essential for mGluR-LTD. Neuron 59, 70–83.
Rajakulendran, S., Hanna, M.G., 2016. The role of calcium channels in epilepsy. Cold Spring Harb. Perspect. Med. 6, a022723.
Reid, H.M., et al., 1983. Hippocampal lesions render SJL/J mice susceptible to audiogenic seizures. Exp. Neurol. 82, 237–240.
Ronesi, J.A., et al., 2012. Disrupted Homer scaffolds mediate abnormal mGluR5 function in a mouse model of fragile X syndrome. Nat. Neurosci. 15 (S1), 431–440.
Russo, E., et al., 2013. Pharmacodynamic potentiation of antiepileptic drugs' effects by some HMG-CoA reductase inhibitors against audiogenic seizures in DBA/2 mice. Pharmacol. Res. 70, 1–12.
Santini, E., Klann, E., 2016. Genetically dissecting cortical neurons involved in epilepsy in Angelman syndrome. Neuron 90, 1–3.
Scheffner, M., et al., 1993. The HPV-16 E6 and E6-AP complex functions as a ubiquitin-protein ligase in the ubiquitination of p53. Cell 75, 495–505.
Scicchitano, F., et al., 2015. Statins and epilepsy: preclinical studies, clinical trials and statin-anticonvulsant drug interactions. Curr. Drug Targets 16, 747–756.
Sell, G.L., Margolis, S.S., 2015. From UBE3A to Angelman syndrome: a substrate perspective. Front. Neurosci. 9, 322.
Shaaya, E.A., et al., 2016. Seizure treatment in Angelman syndrome: a case series from the Angelman Syndrome Clinic at Massachusetts General Hospital. Epilepsy Behav. 60, 138–141.
Sidorov, M.S., et al., 2017. Delta rhythmicity is a reliable EEG biomarker in Angelman syndrome: a parallel mouse and human analysis. J. Neurodev. Disord. 9, 17.
Stasheff, S.F., et al., 1989. NMDA antagonists differentiate epileptogenesis from seizure expression in an in vitro model. Science 245, 648–651.
Stiglbauer, V., et al., 2017. Cav 1.3 channels play a crucial role in the formation of paroxysmal depolarization shifts in cultured hippocampal neurons. Epilepsia 58, 858–871.
Sun, J., et al., 2015. UBE3A regulates synaptic plasticity and learning and memory by controlling SK2 channel endocytosis. Cell Rep. 12, 449–461.
Tan, W.H., Bird, L.M., 2016. Angelman syndrome: current and emerging therapies in 2016. Am. J. Med. Genet. C: Semin. Med. Genet. 172, 384–401.
Taylor, G.W., et al., 1995. Synchronized oscillations in hippocampal CA3 neurons induced by metabotropic glutamate receptor activation. J. Neurosci. 15, 8039–8052.
Thibert, R.L., et al., 2009. Epilepsy in Angelman syndrome: a questionnaire-based assessment of the natural history and current treatment options. Epilepsia 50, 2369–2376.
Thibert, R.L., et al., 2013. Neurologic manifestations of Angelman syndrome. Pediatr. Neurol. 48, 271–279.
Thomson, S.R., et al., 2017. Cell-type-specific translation profiling reveals a novel strategy for treating fragile X syndrome. Neuron 95, 550-563.e5.
Vendrame, M., et al., 2012. Analysis of EEG patterns and genotypes in patients with Angelman syndrome. Epilepsy Behav. 23, 261–265.
Wallace, M.L., et al., 2012. Maternal loss of Ube3a produces an excitatory/inhibitory imbalance through neuron type-specific synaptic defects. Neuron 74, 793–800.
van Woerden, G.M., et al., 2007. Rescue of neurological deficits in a mouse model for Angelman syndrome by reduction of alphaCaMKII inhibitory phosphorylation. Nat. Neurosci. 10, 280–282.
Yashiro, K., et al., 2009. Ube3a is required for experience-dependent maturation of the neocortex. Nat. Neurosci. 12, 777–783.
Young, S.R., et al., 2013. Persistent receptor activity underlies group I mGluR-mediated cellular plasticity in CA3 neuron. J. Neurosci. 33, 2526–2540.
Zamponi, G.W., et al., 2015. The physiology, pathology, and pharmacology of voltage-gated calcium channels and their future therapeutic potential. Pharmacol. Rev. 67, 821–870.
Zhao, W., et al., 2004. Extracellular signal-regulated kinase 1/2 is required for the induction of group I metabotropic glutamate receptor-mediated epileptiform discharges. J.Neurosci. 24, 76–84.
Zhao, W., et al., 2015. Extracellular glutamate exposure facilitates group I mGluR-mediated epileptogenesis in the hippocampus. J. Neurosci. 35, 308–315.